Published in "ChemPhysChem 16(3): 649–657, 2015"
which should be cited to refer to this work.

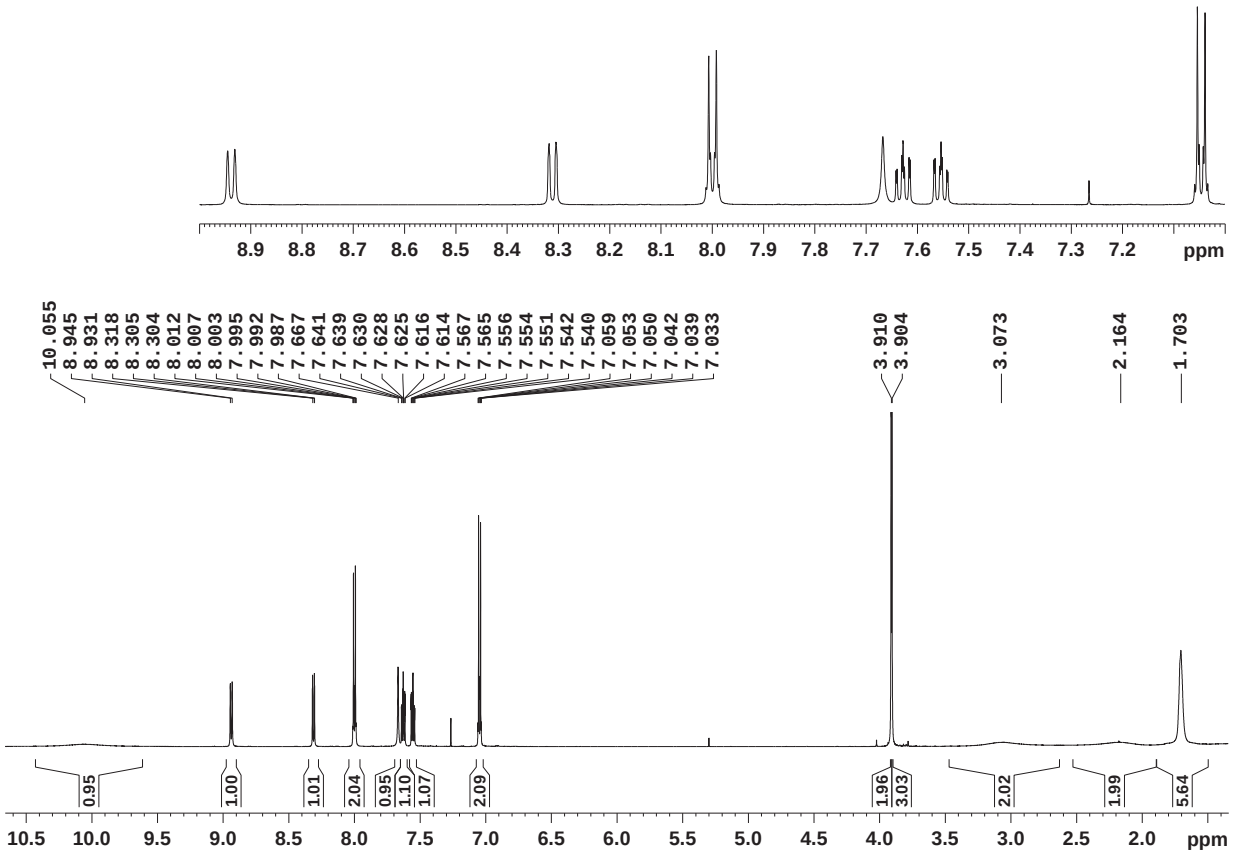

Figure S1. ^{1}H NMR spectrum of **2**.

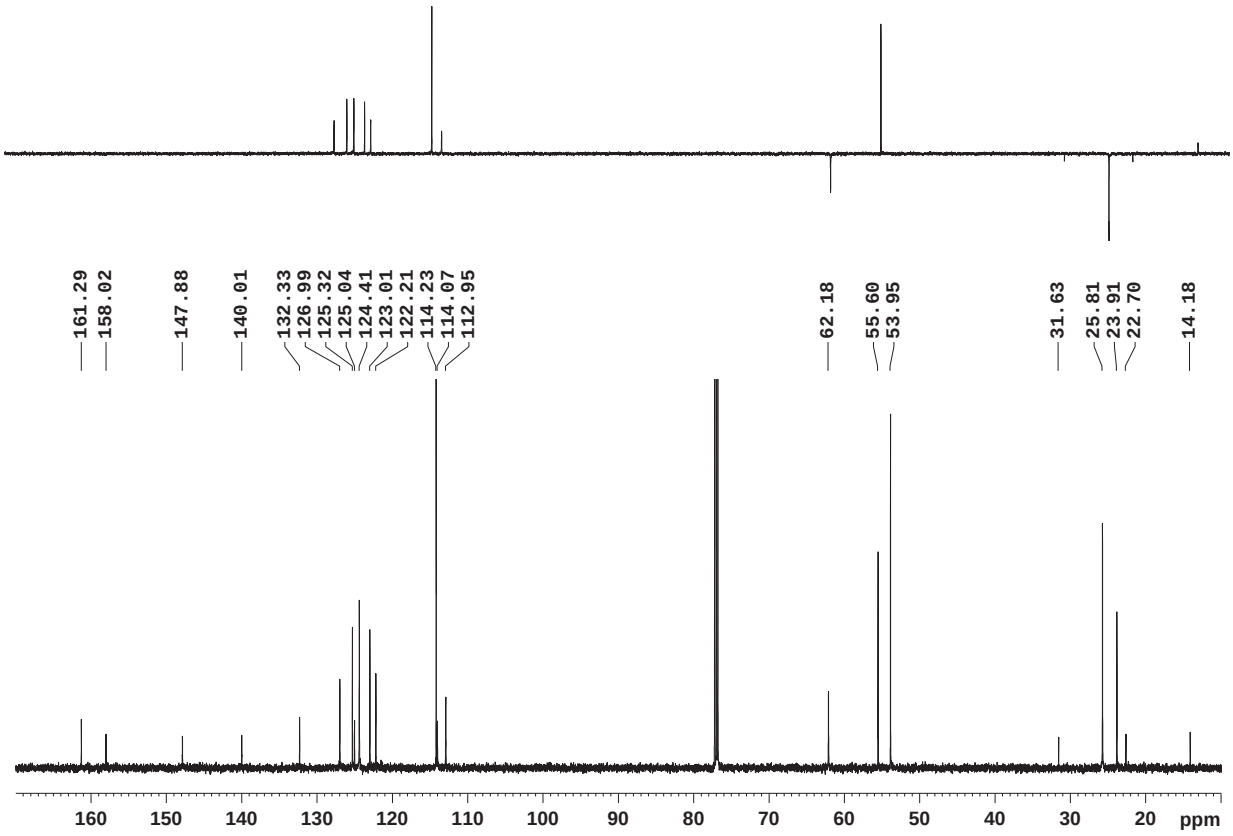

Figure S2. ^{13}C (down) and DEPT (up) NMR spectra of **2**.

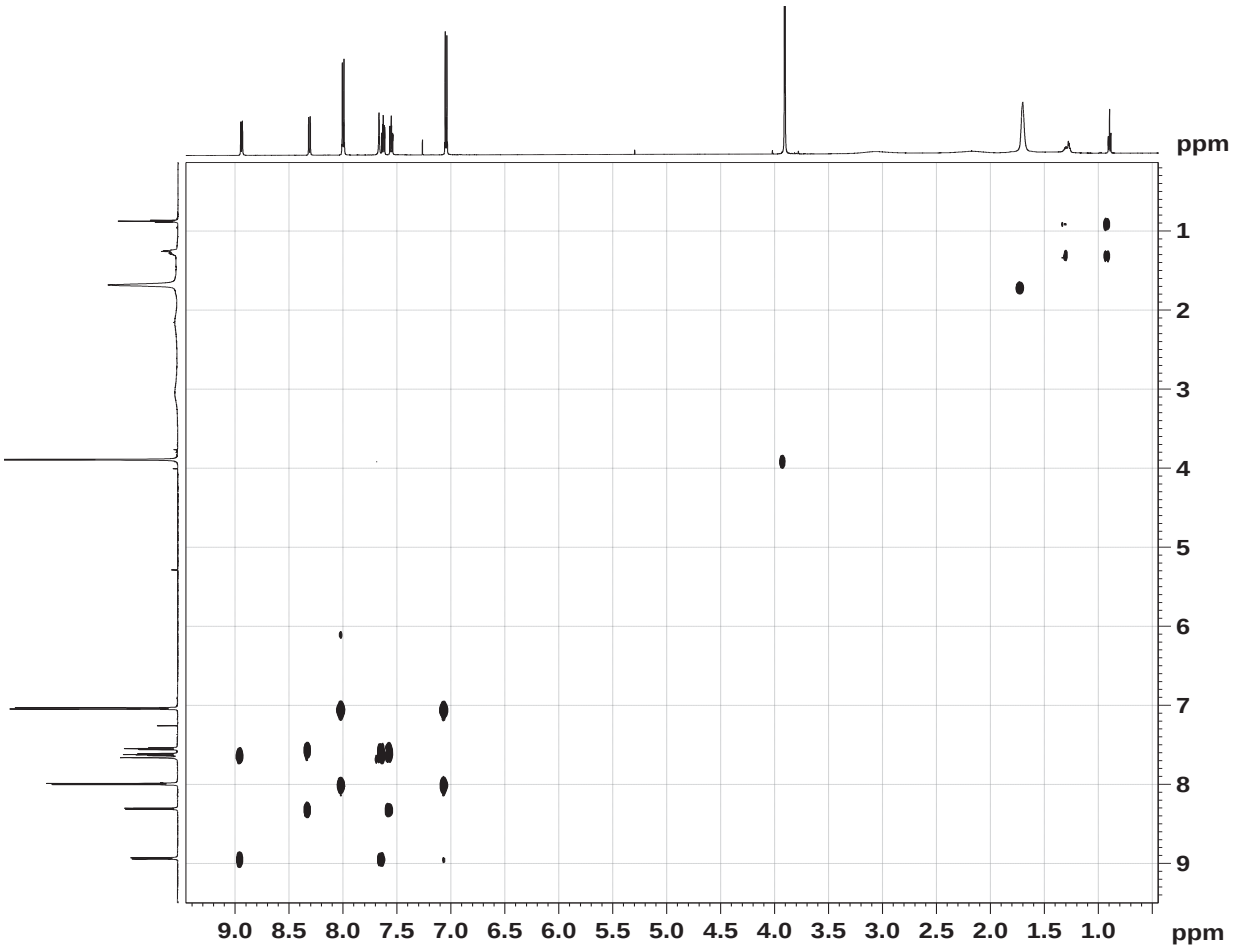

Figure S3. ^{1}H-^{1}H COSY NMR experiment of **2**.

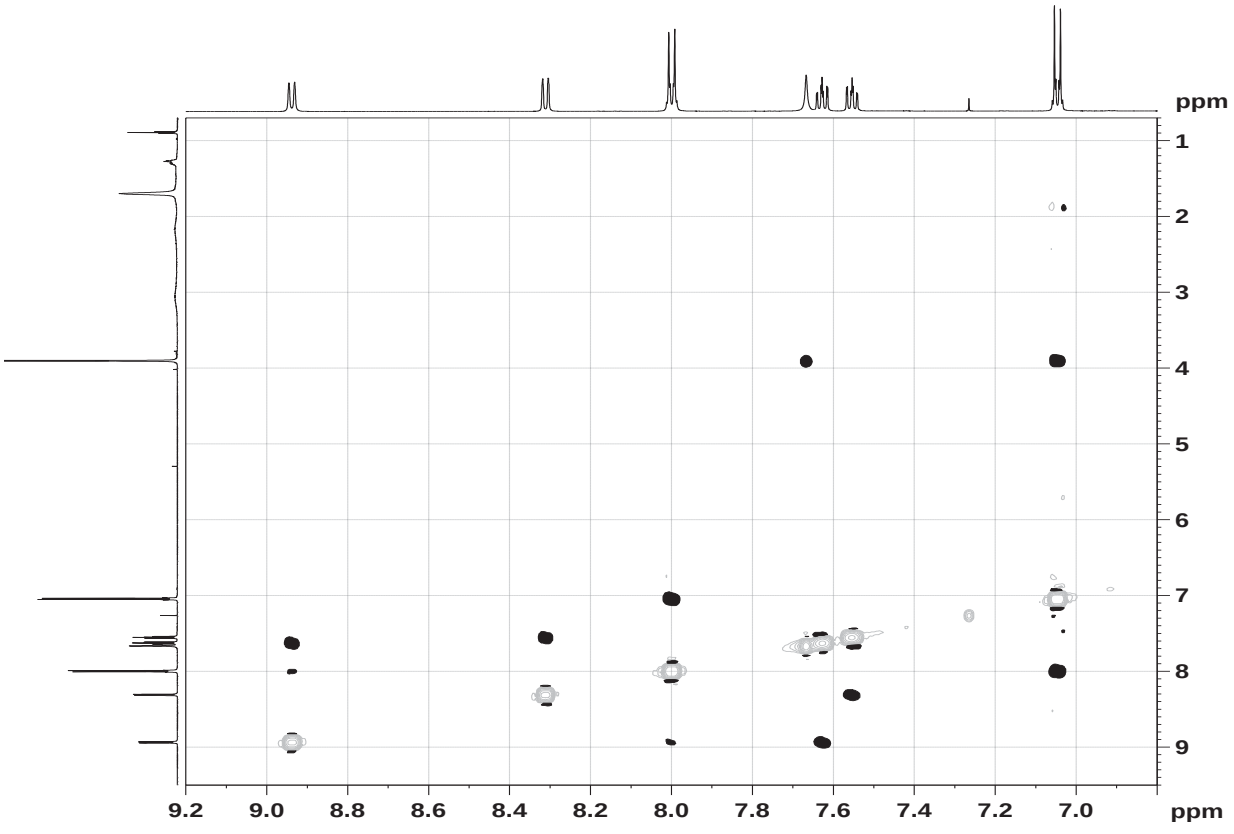

Figure S4. ^{1}H-^{1}H NOESY NMR experiment of **2**.

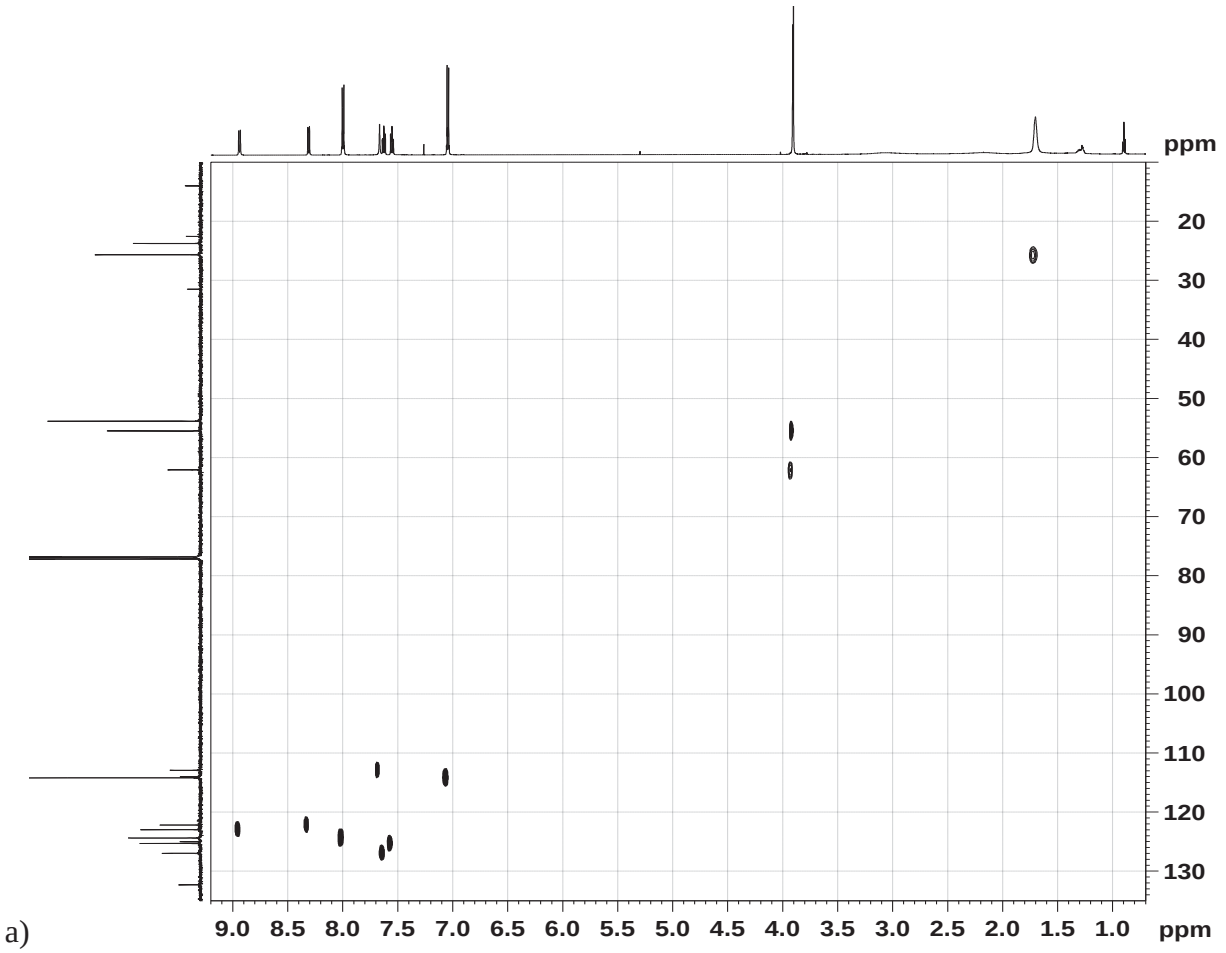

a)

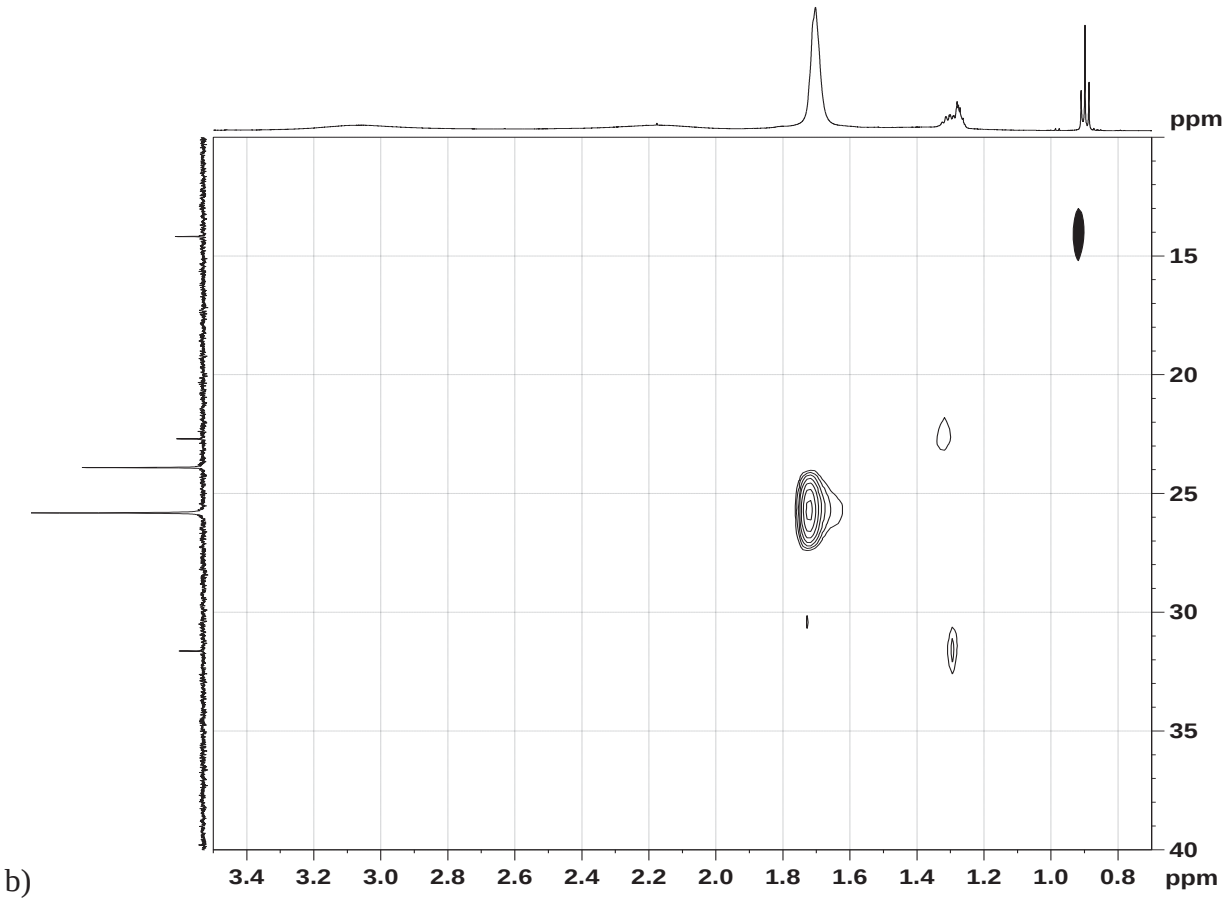

b)

Figure S5. ^{1}H-^{13}C HSQC NMR experiment of **2**: a) full spectrum; b) aliphatic part.

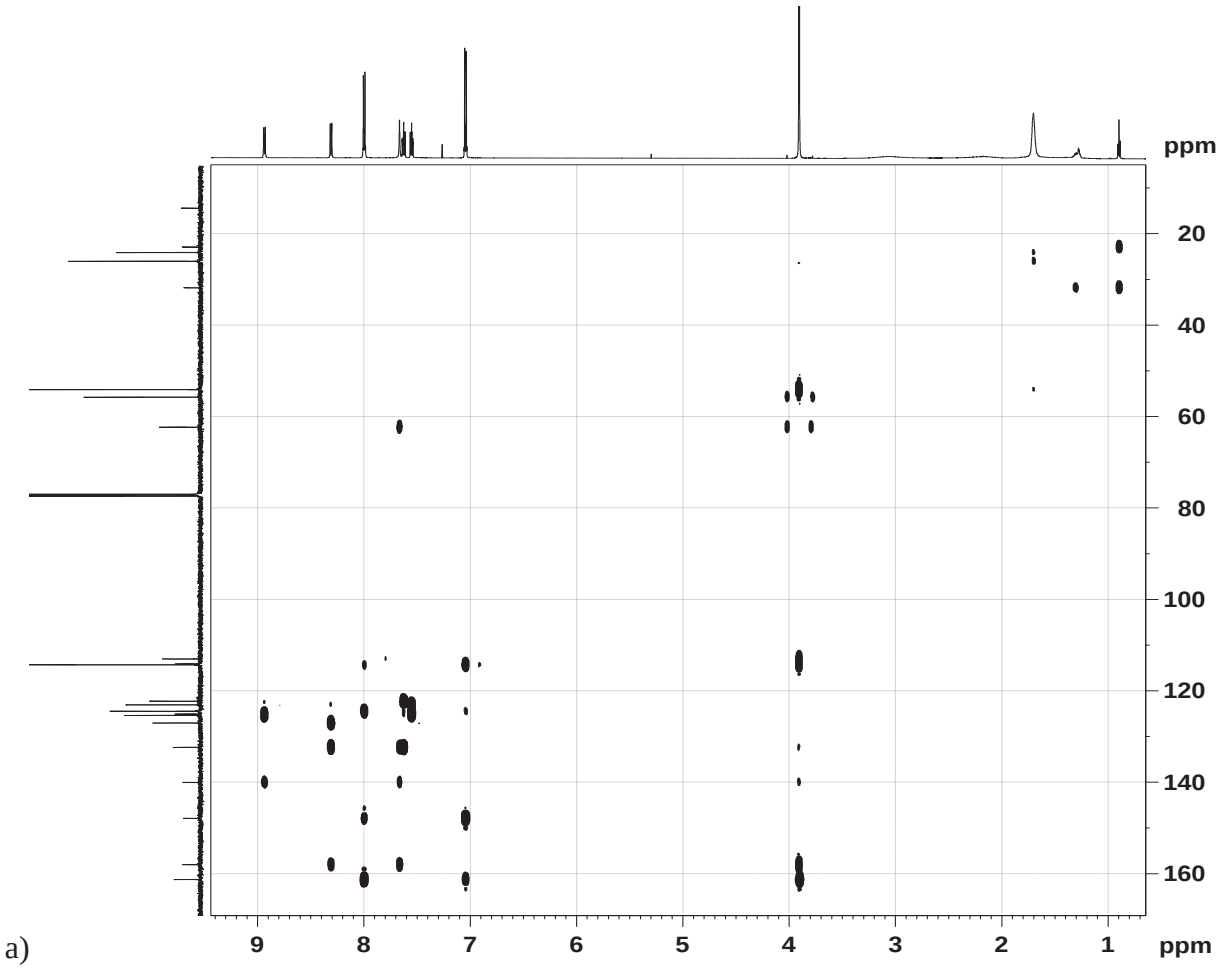

a)

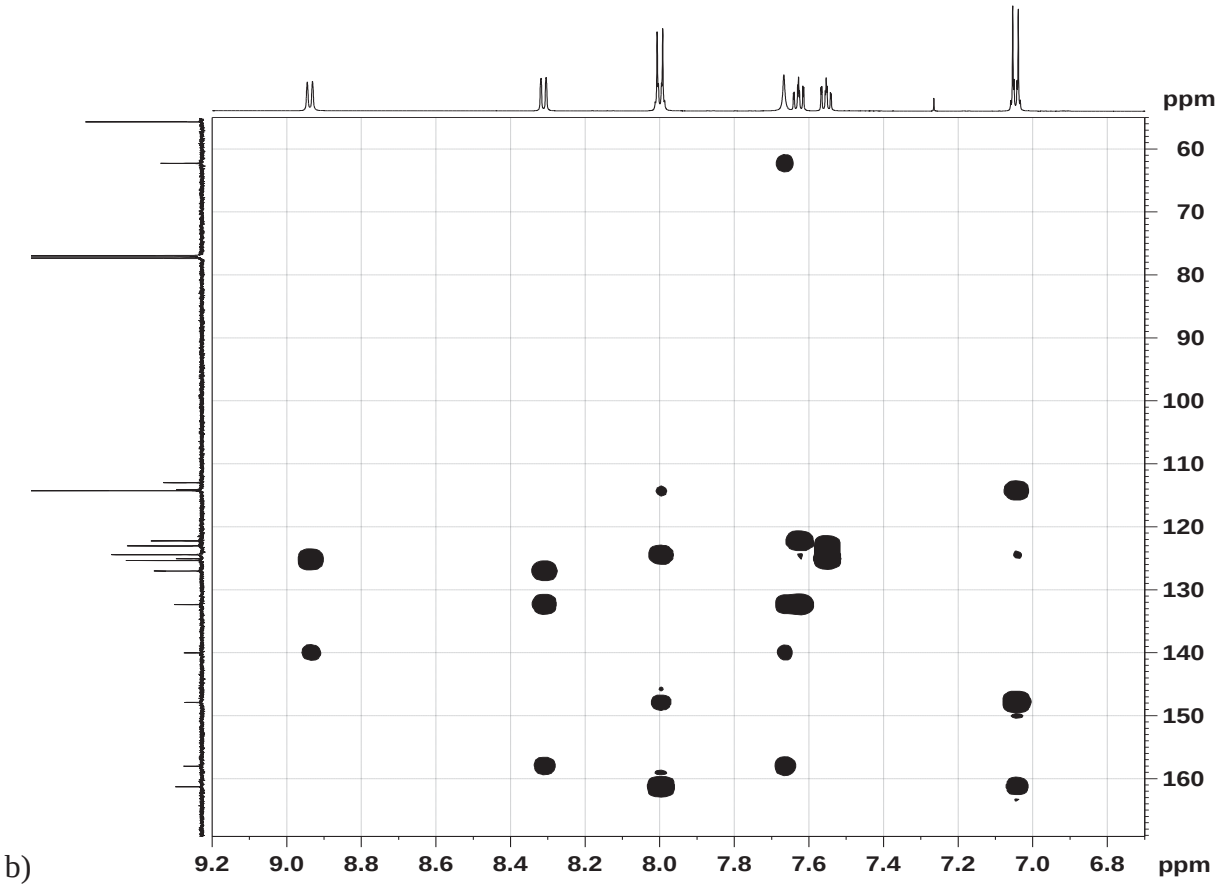

b)

Figure S6. ^{1}H-^{13}C HMBC NMR experiment of **2**: a) full spectrum; b) aromatic part.

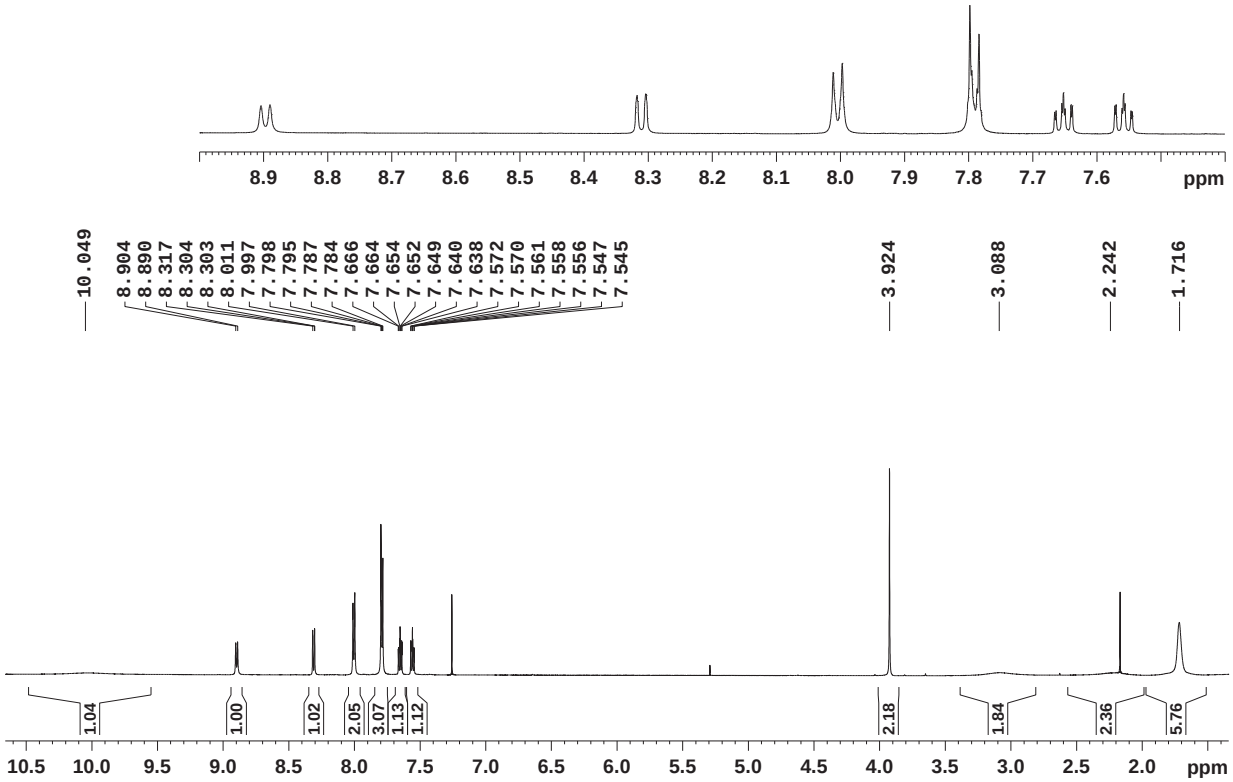

Figure S7. ^{1}H NMR spectrum of **3**.

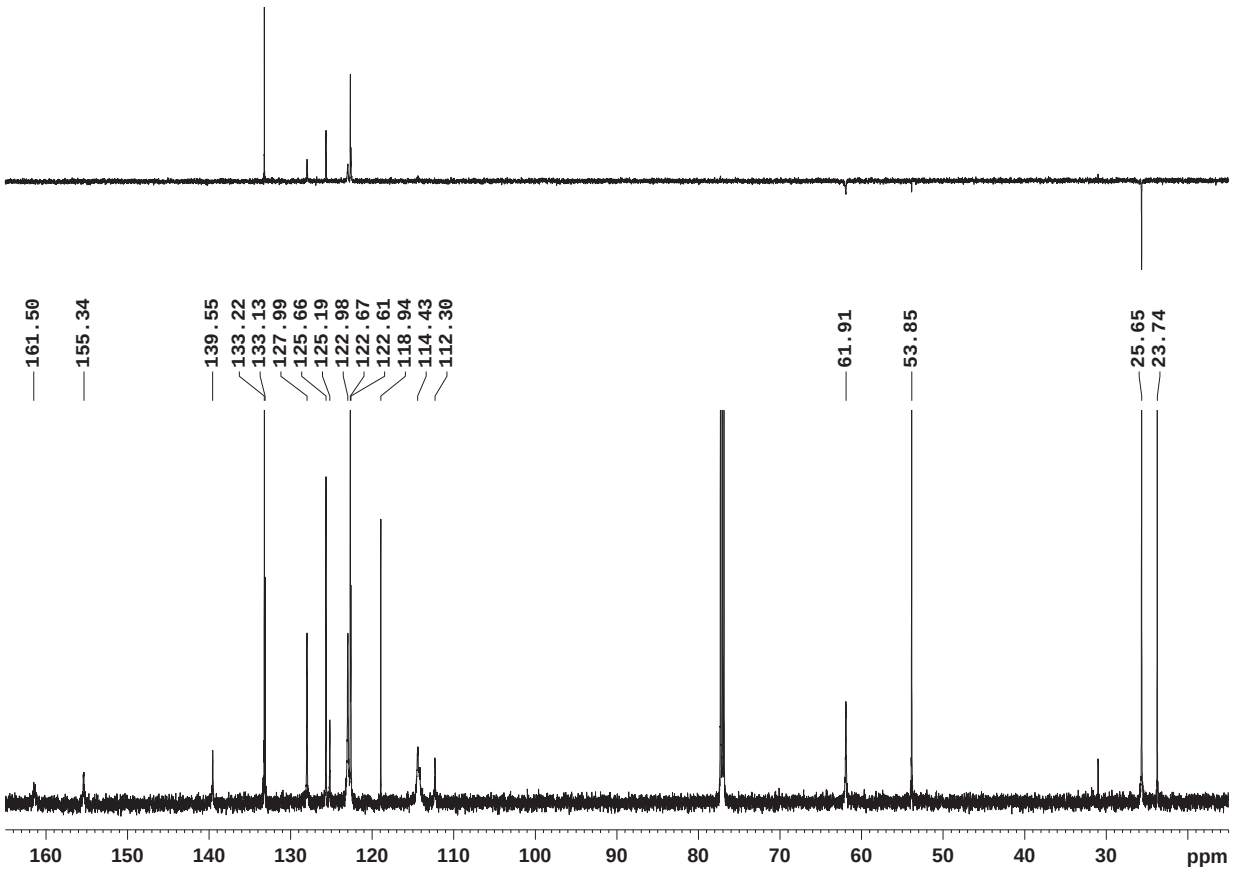

Figure S8. ^{13}C (down) and DEPT (up) NMR spectra of **3**.

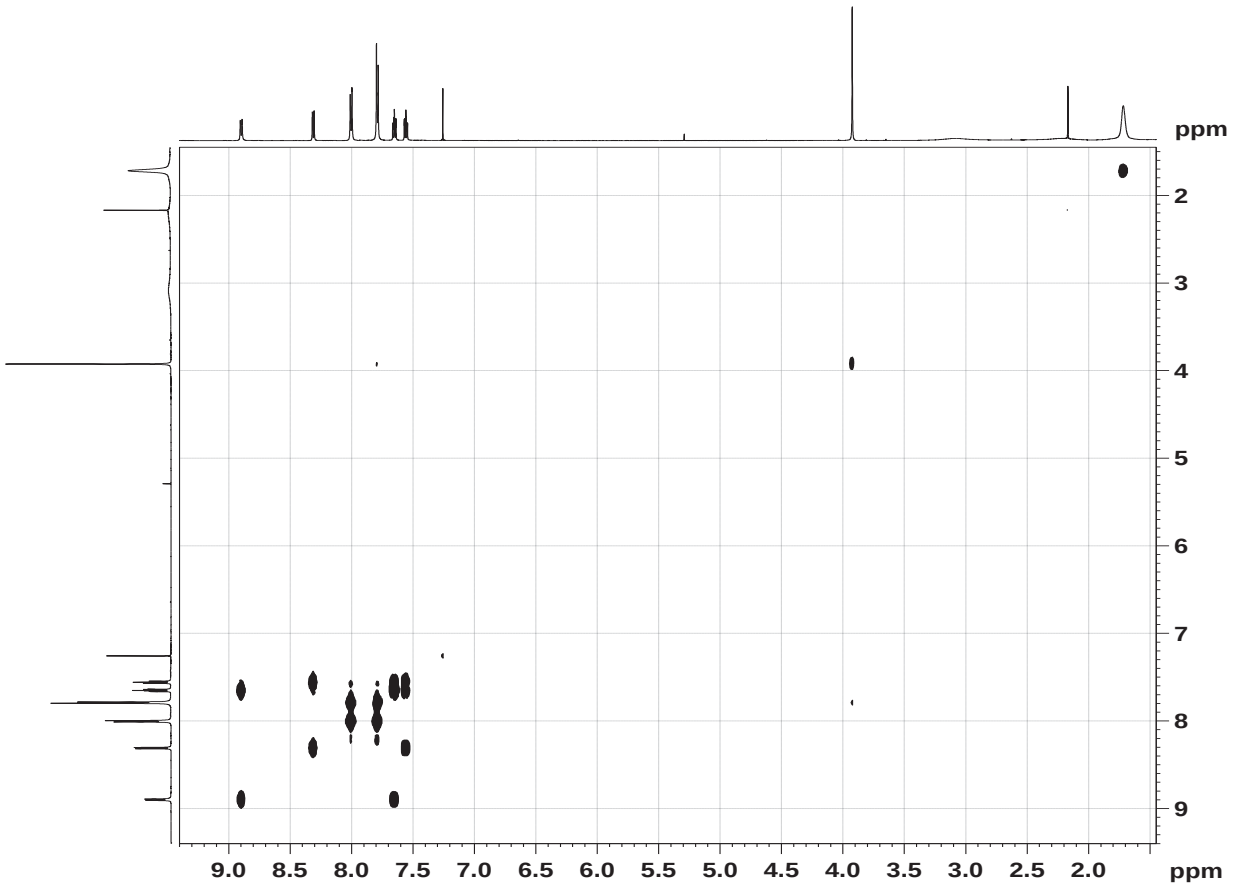

Figure S9. ^{1}H-^{1}H COSY NMR experiment of **3**.

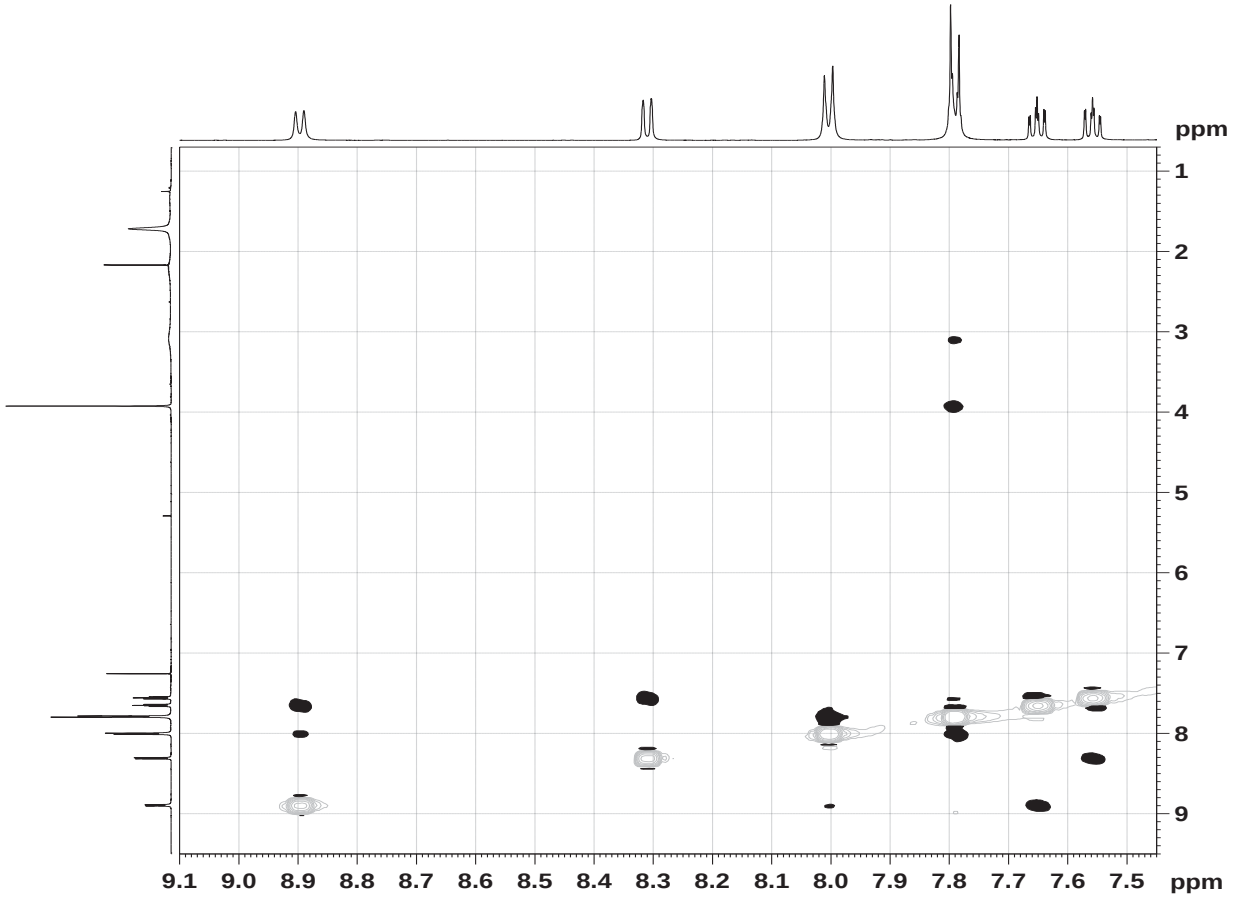

Figure S10. ^{1}H-^{1}H NOESY NMR experiment of **3**.

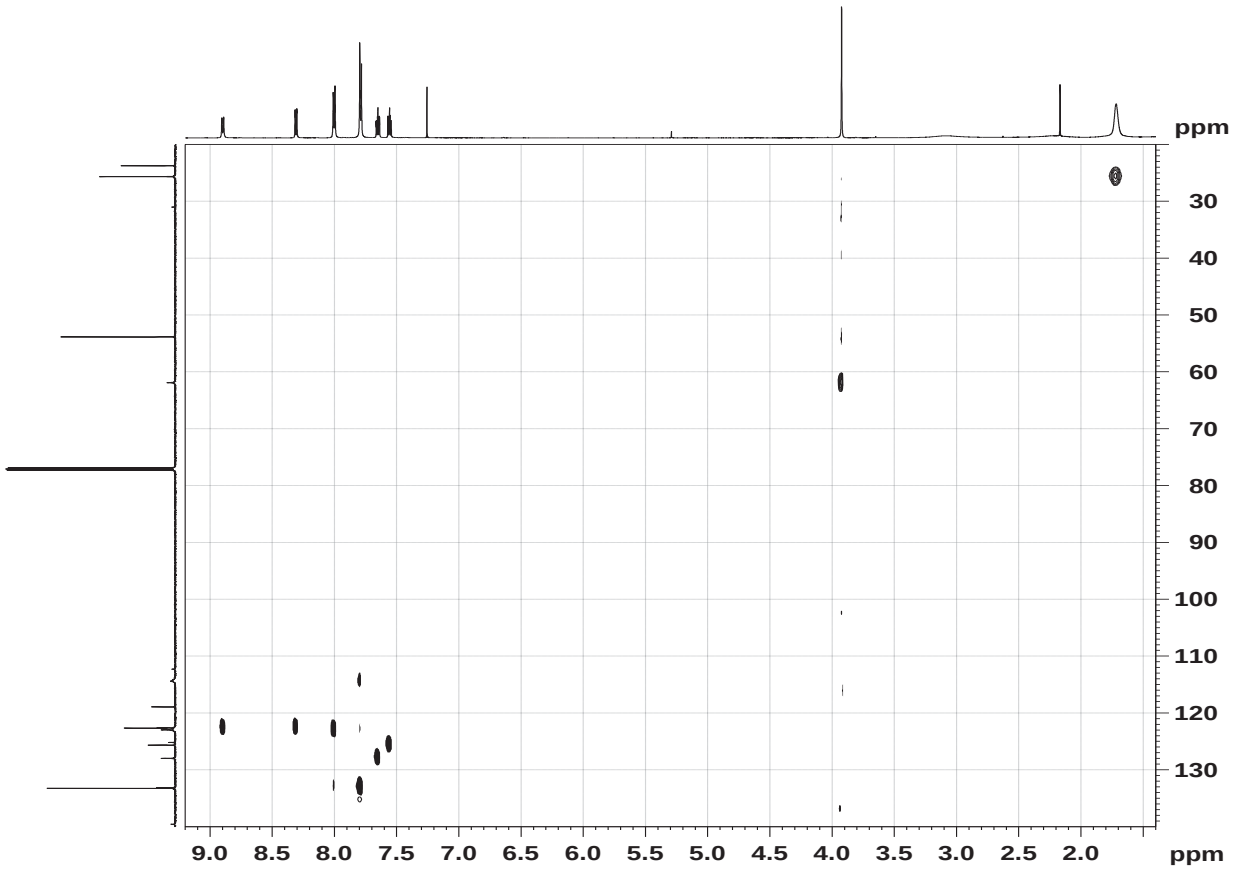

Figure S11. ^{1}H-^{13}C HSQC NMR experiment of **3**.

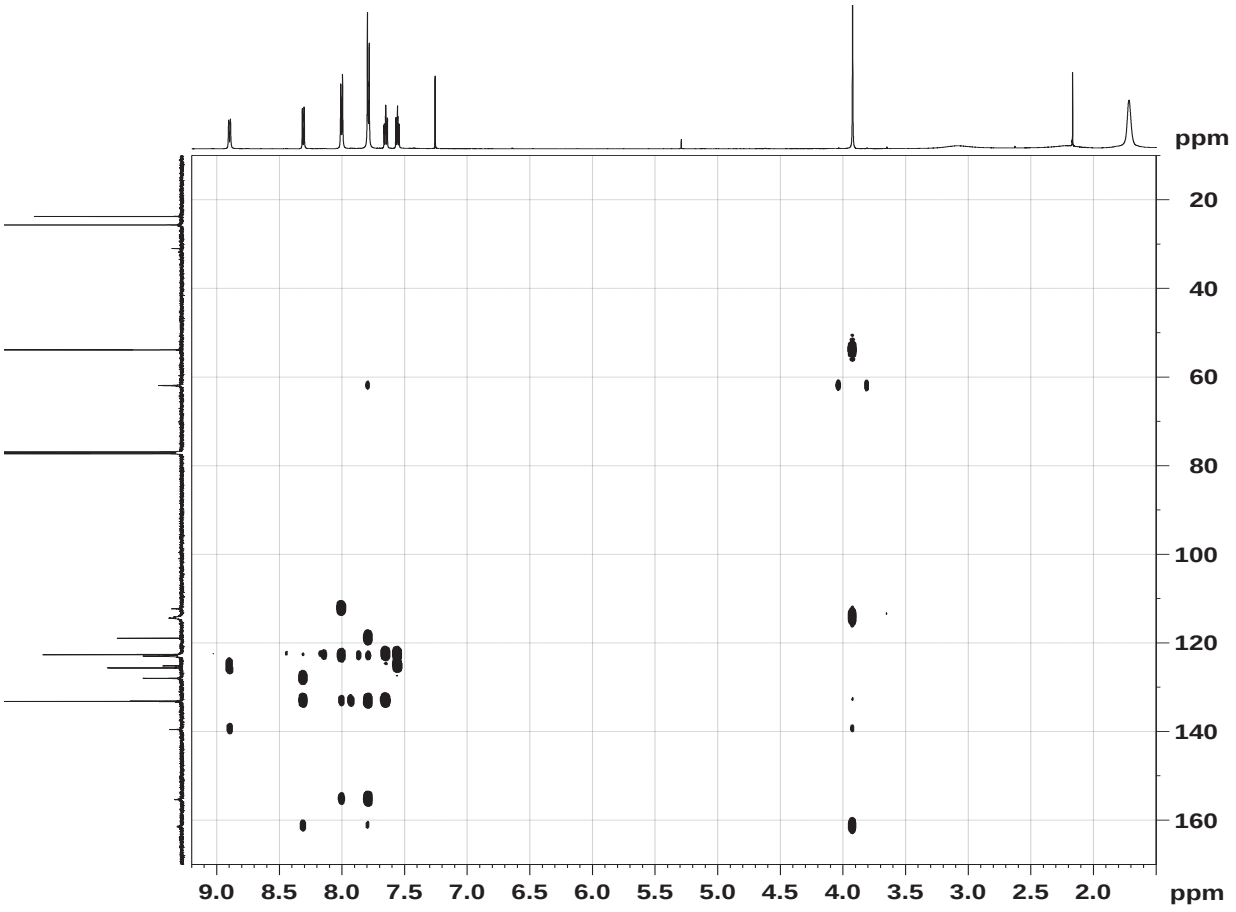

Figure S12. ^{1}H-^{13}C HMBC NMR experiment of **3**.

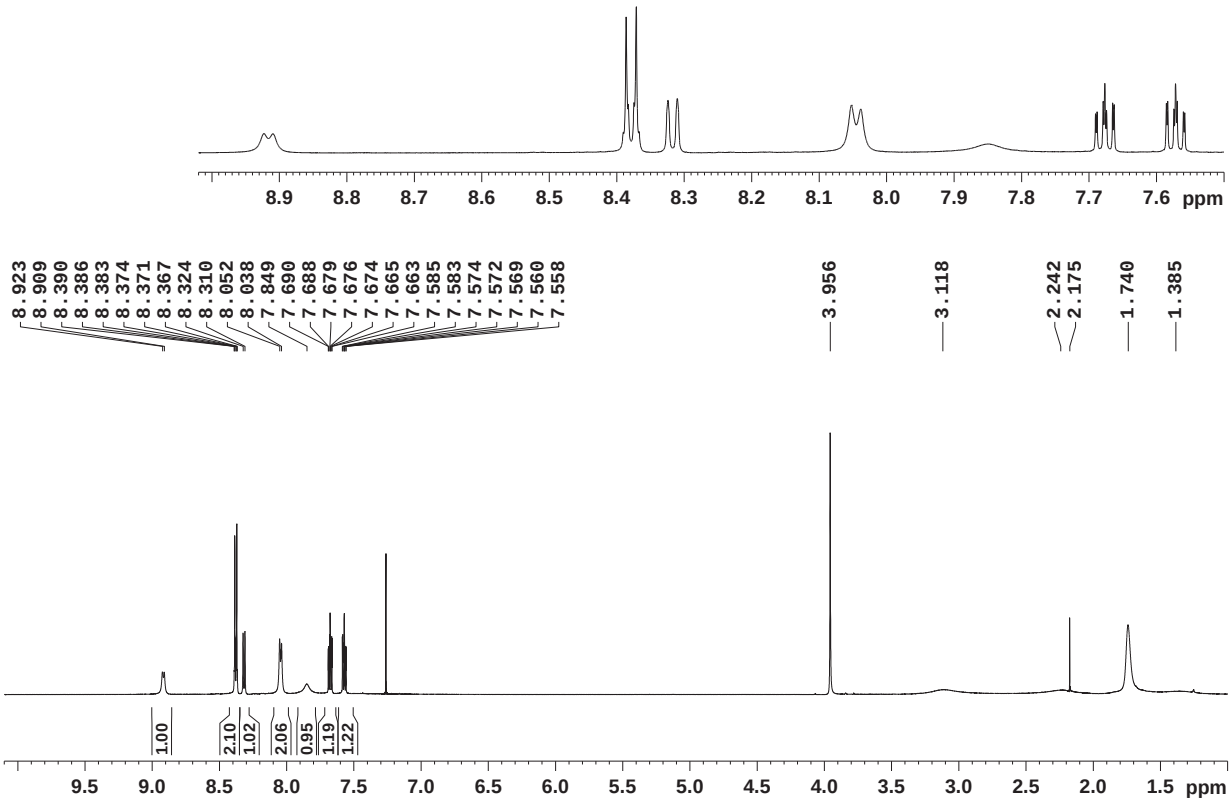

Figure S13. ^{1}H NMR spectrum of **4**.

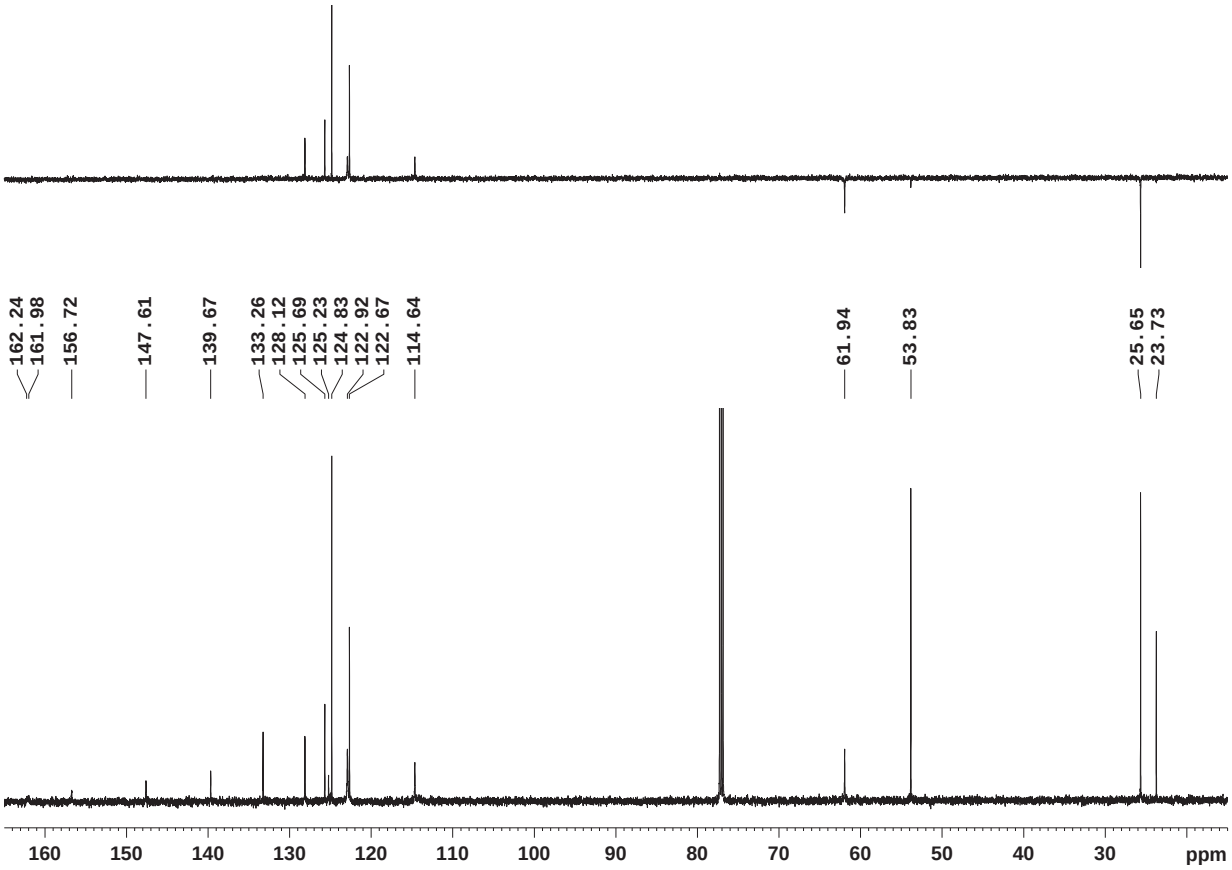

Figure S14. ^{13}C (down) and DEPT (up) NMR spectra of **4**.

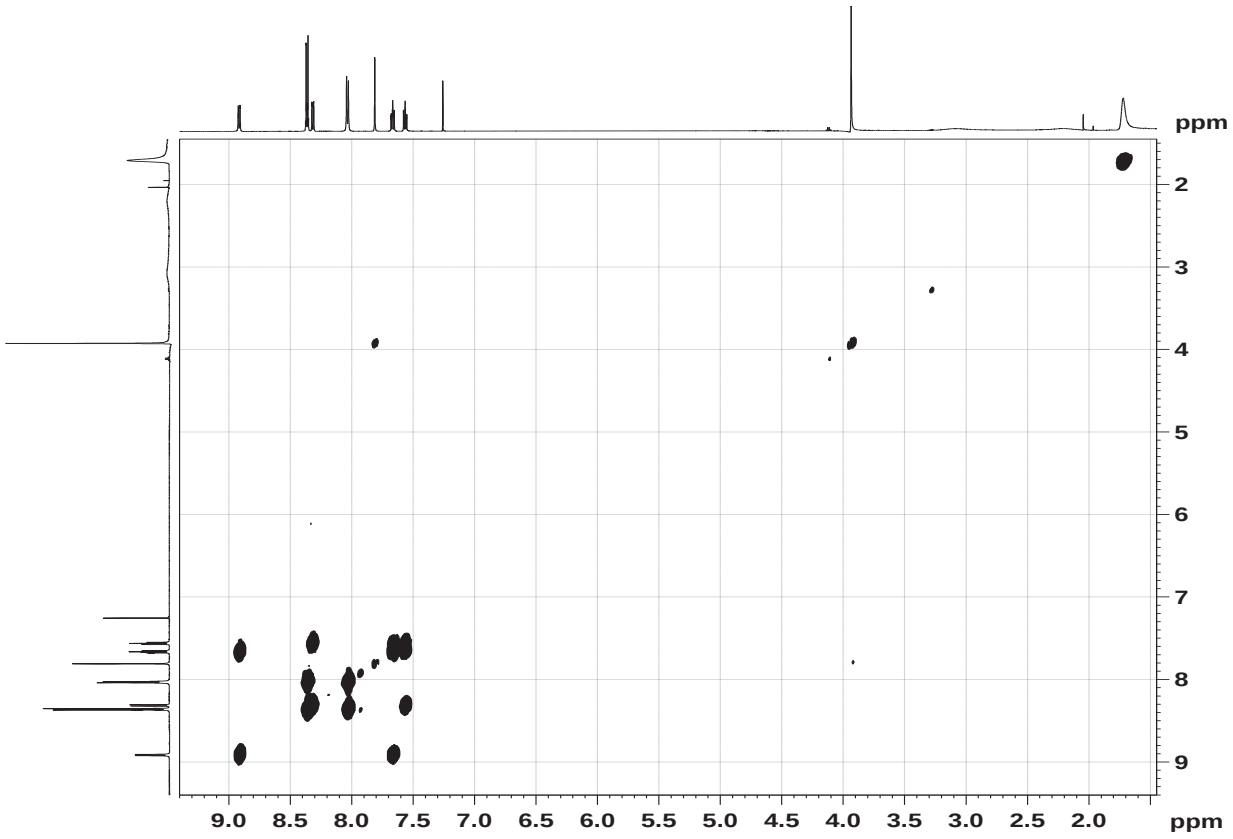

Figure S15. ^{1}H-^{1}H COSY NMR experiment of **4**.

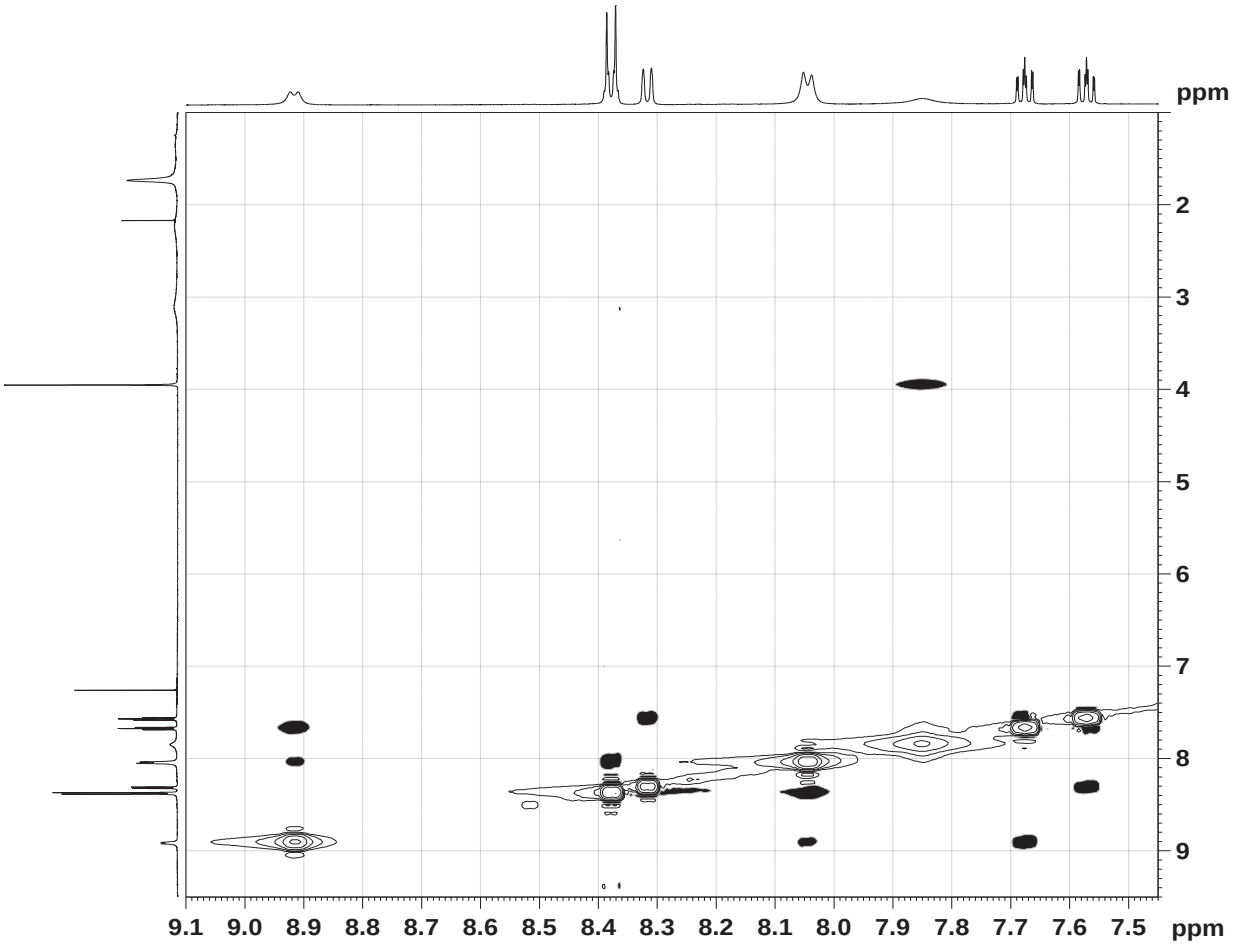

Figure S16. ^{1}H-^{1}H NOESY NMR experiment of **4**.

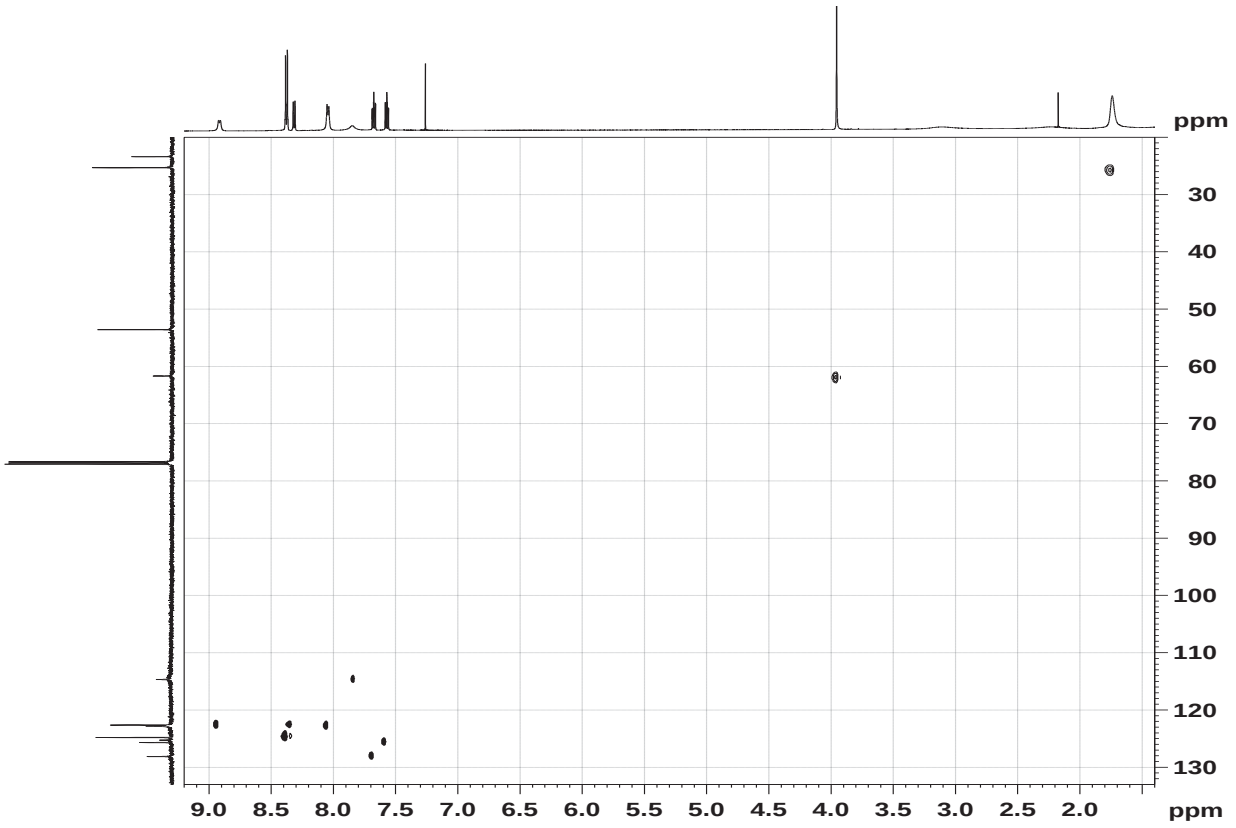

Figure S17. ^{1}H-^{13}C HSQC NMR experiment of **4**.

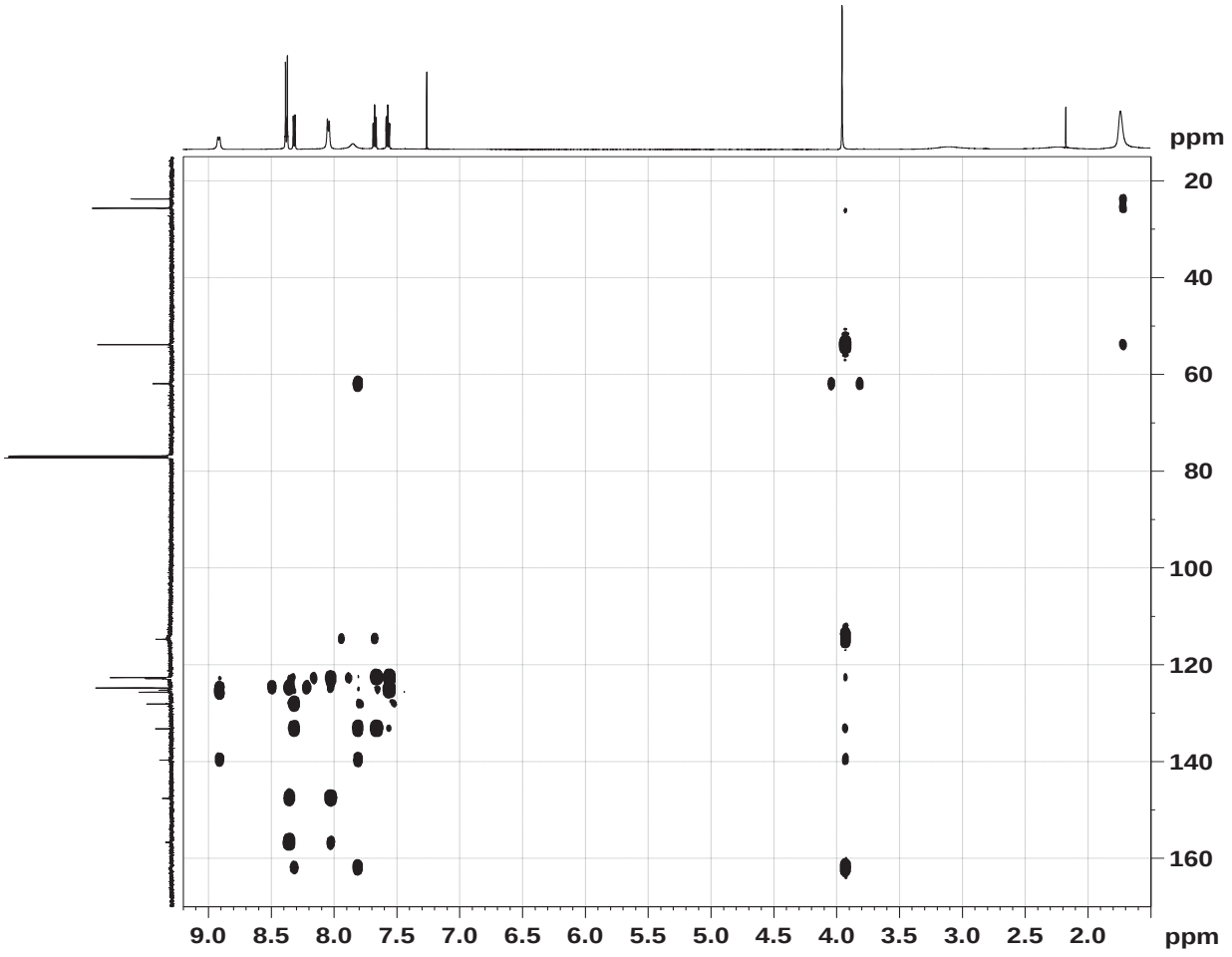

Figure S18. ^{1}H-^{13}C HMBC NMR experiment of **4**.

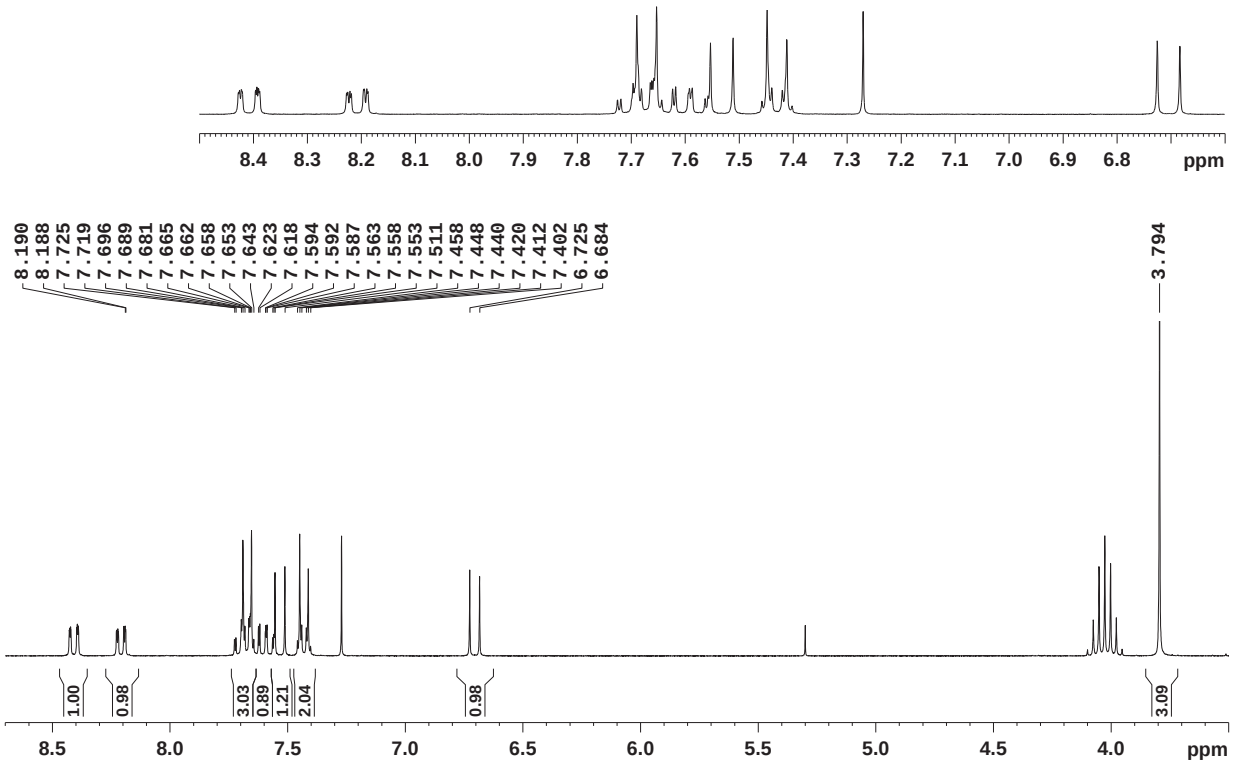

Figure S19. ^{1}H NMR spectrum of **7-NMe** (contains i-PrOH).

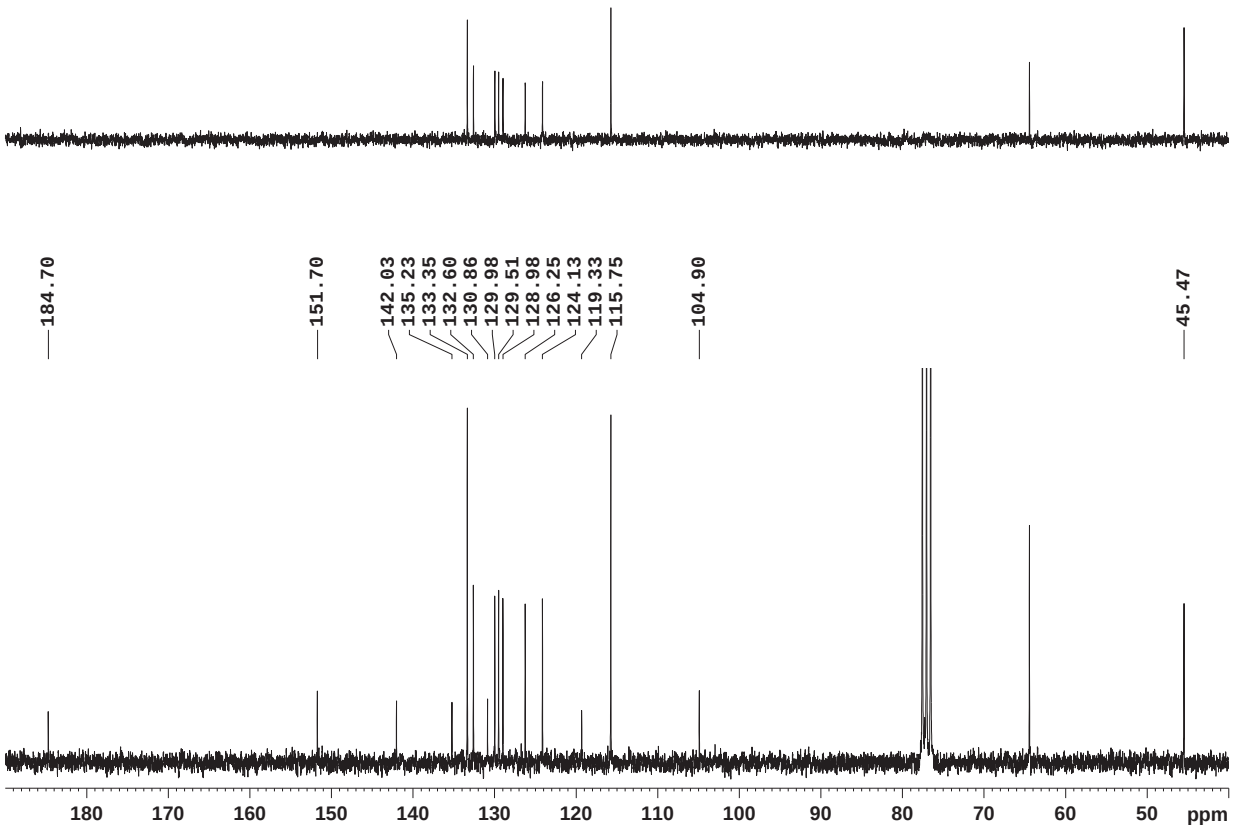

Figure S20. ^{13}C (down) and DEPT (up) NMR spectra of **7-NMe** (contains i-PrOH).

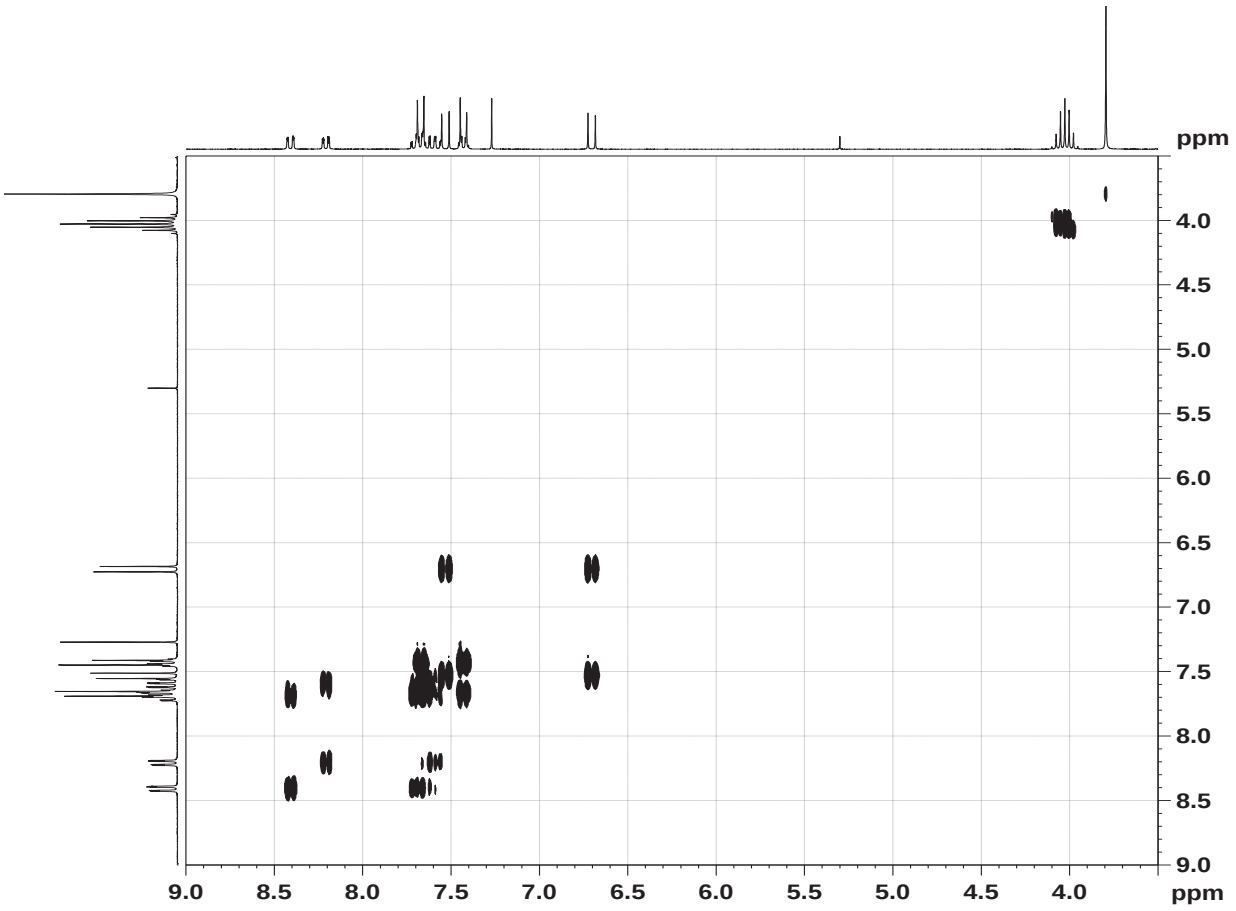

Figure S21. ^{1}H-^{1}H COSY NMR experiment of **7-NMe** (contains i-PrOH).

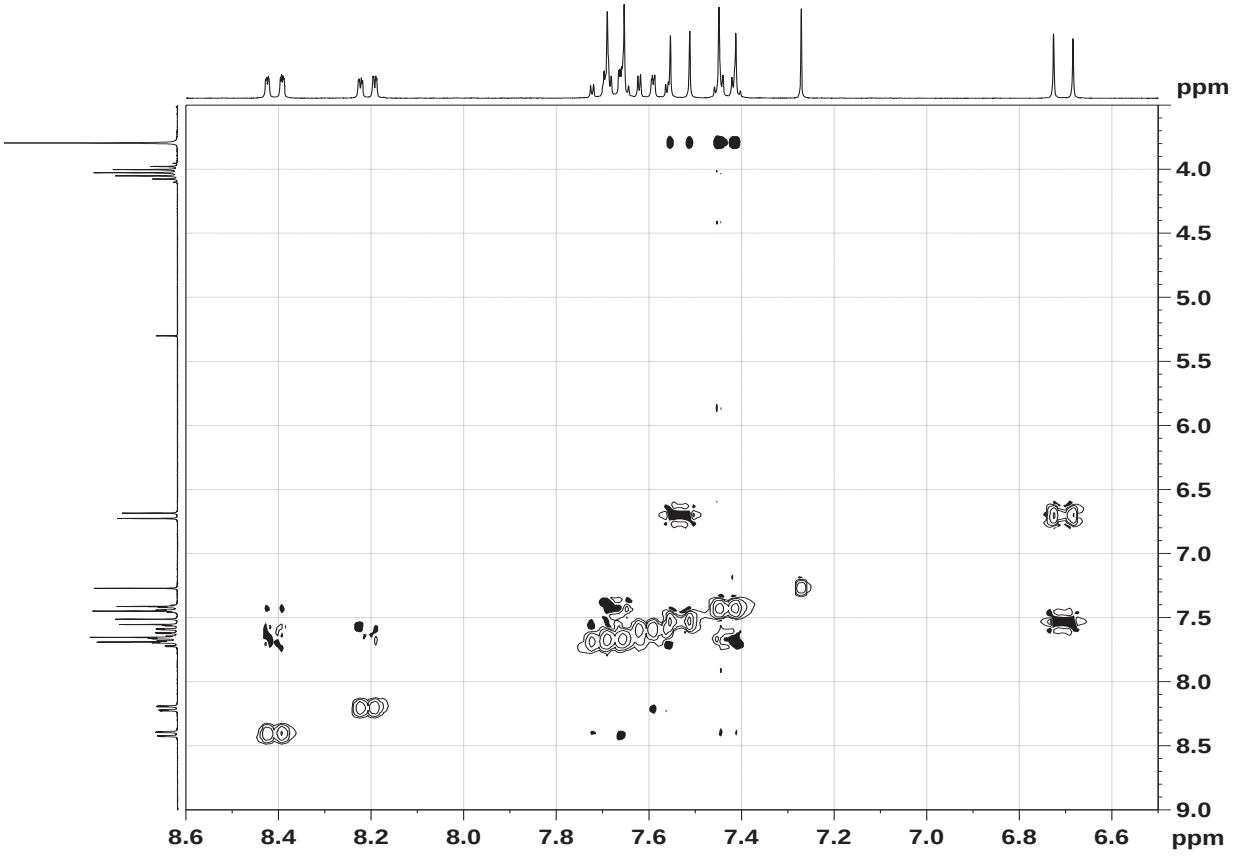

Figure S22. ^{1}H-^{1}H NOESY NMR experiment of **7-NMe** (contains i-PrOH).

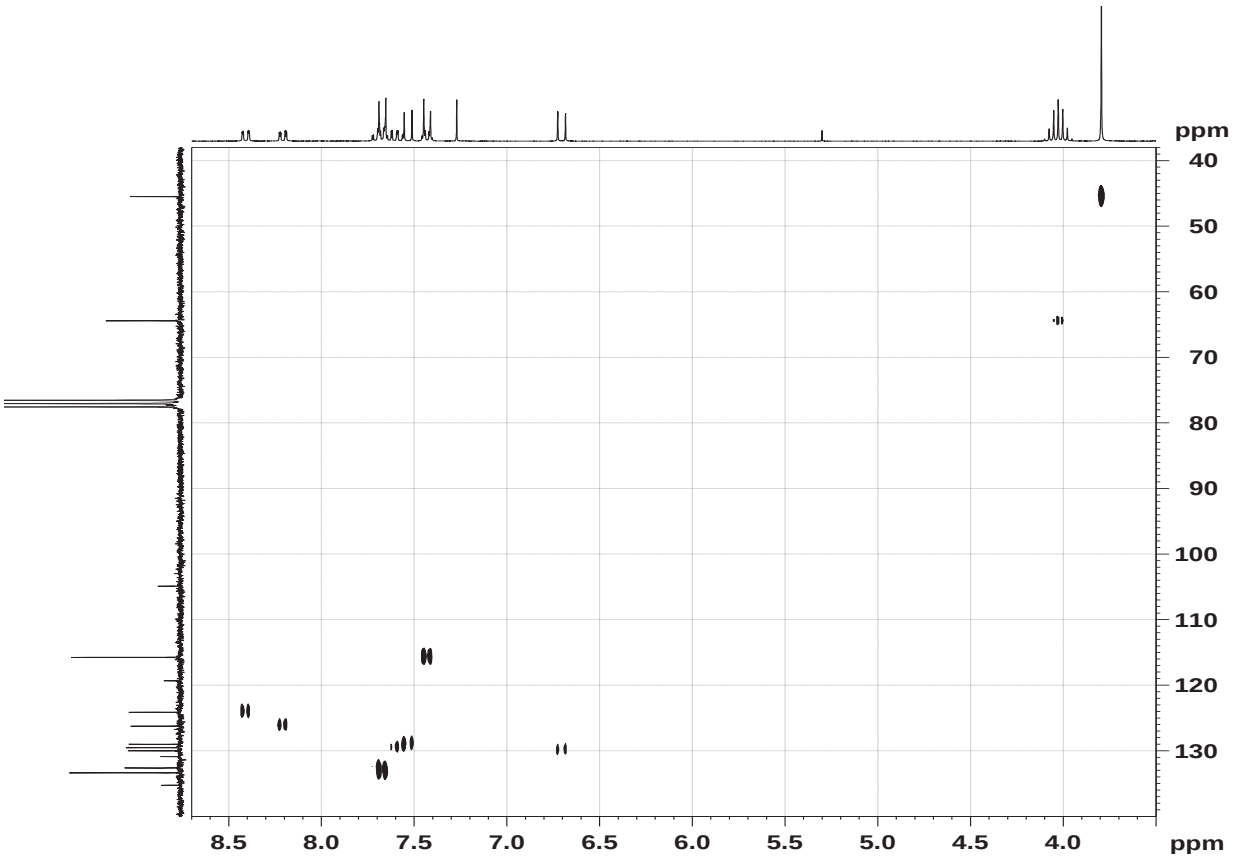

Figure S23. ^{1}H-^{13}C HSQC NMR experiment of **7-NMe** (contains i-PrOH).

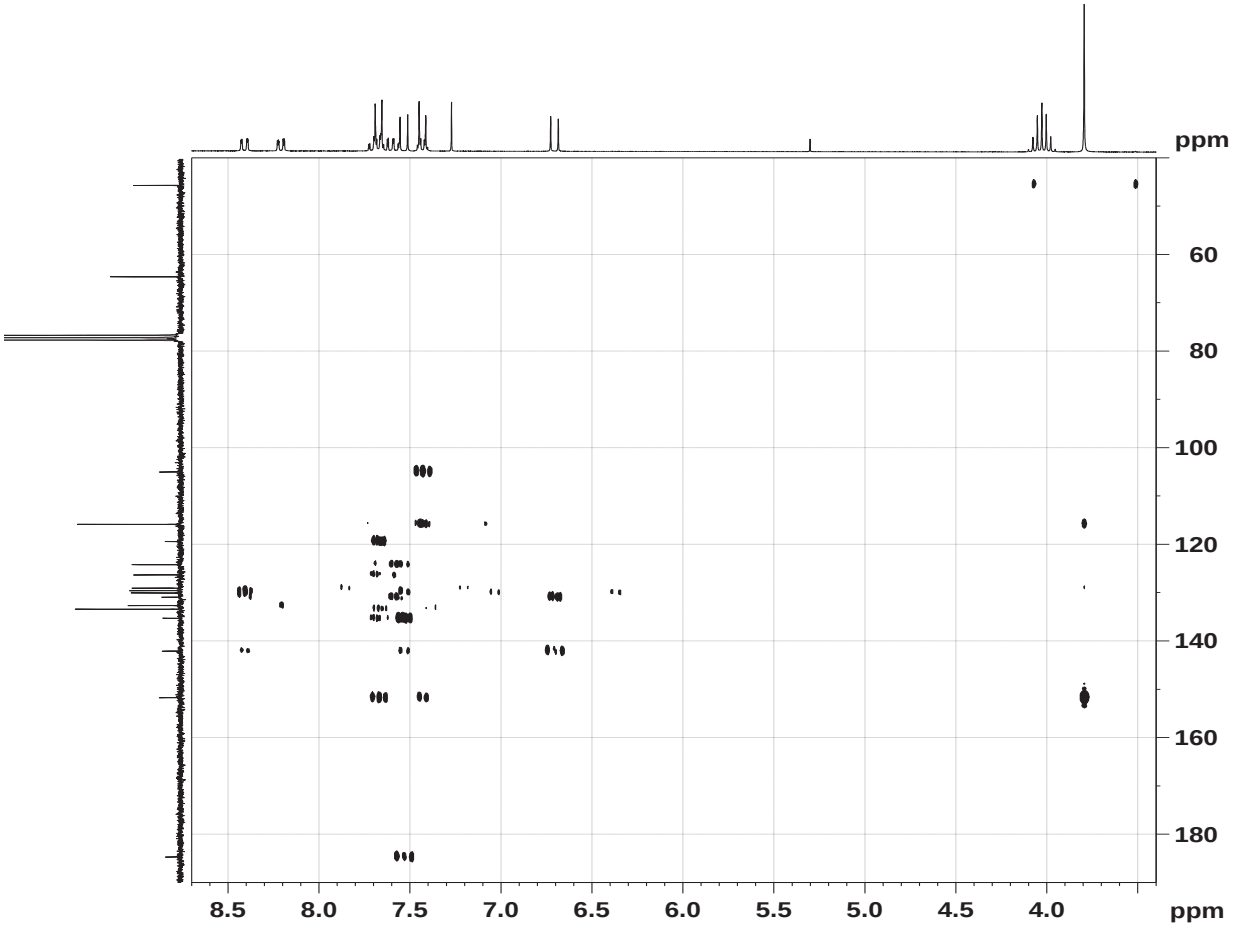

Figure S24. ^{1}H-^{13}C HMBC NMR experiment of **7-NMe** (contains i-PrOH).

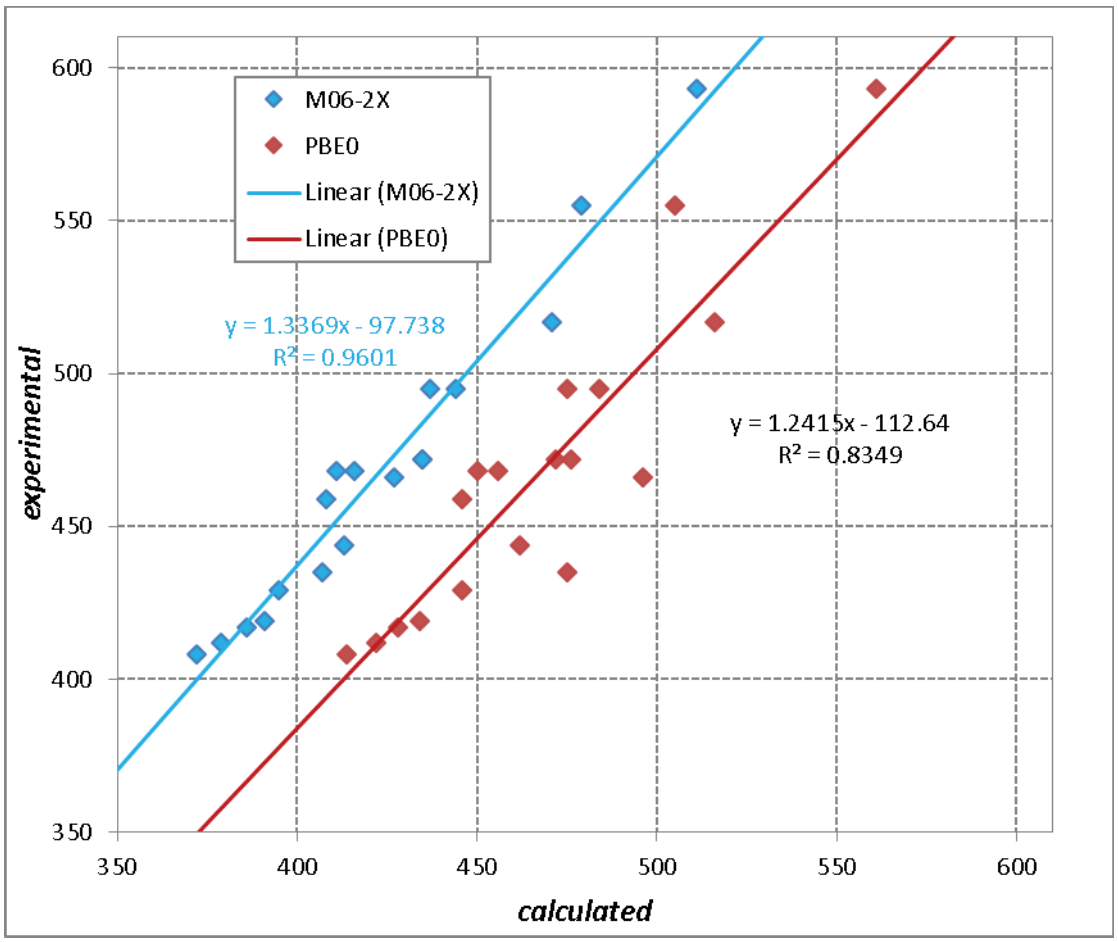

Figure S25. Linearity between experimental and predicted long wavelength absorption maxima in acetonitrile. The values are collected in Tables 1 and S2.

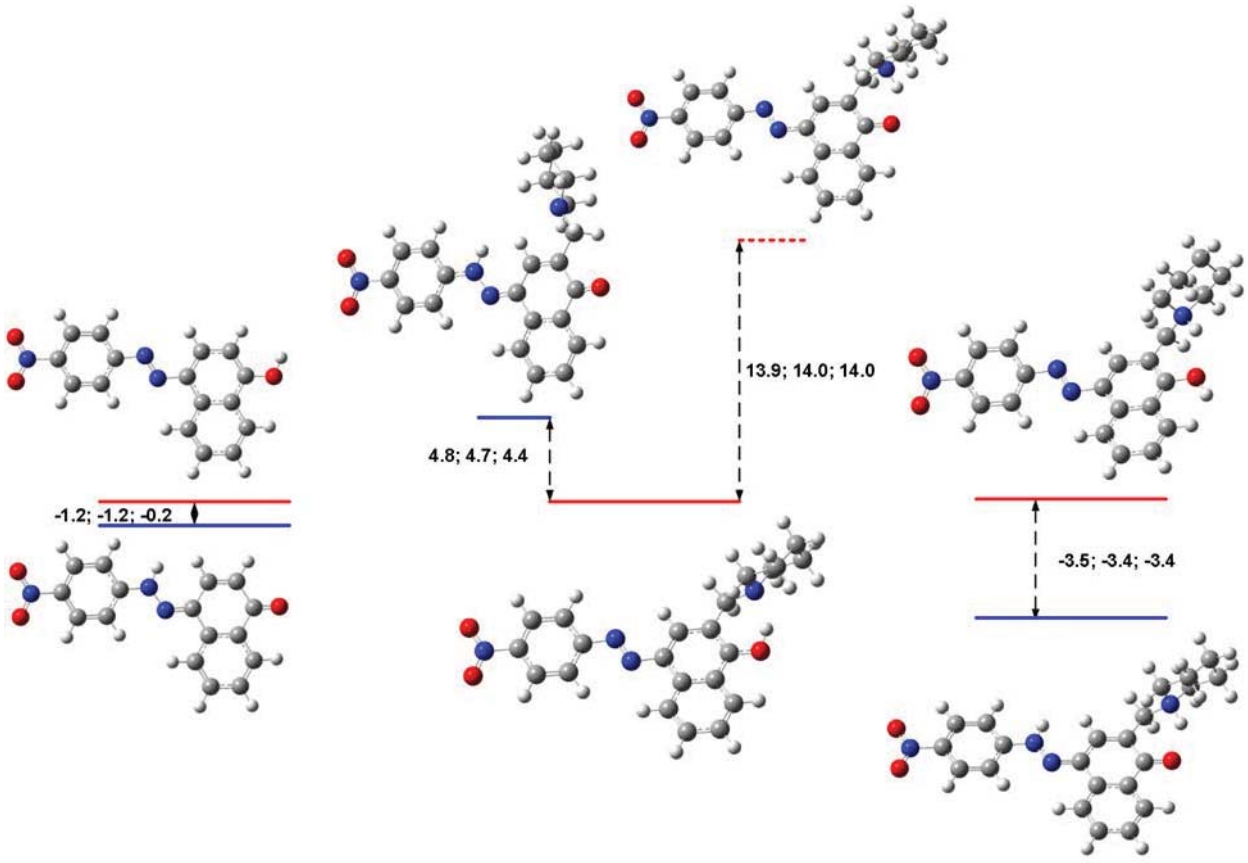

Figure S26: Change of the relative energy (M06-2X/def2-TZVP) of the tautomers in gas phase of the parent compound **8** (left), **4** (center) and **4H**$^+$ (right). The values of ΔE, ΔE+ZPE and ΔΔG are given in kcal/mol units.

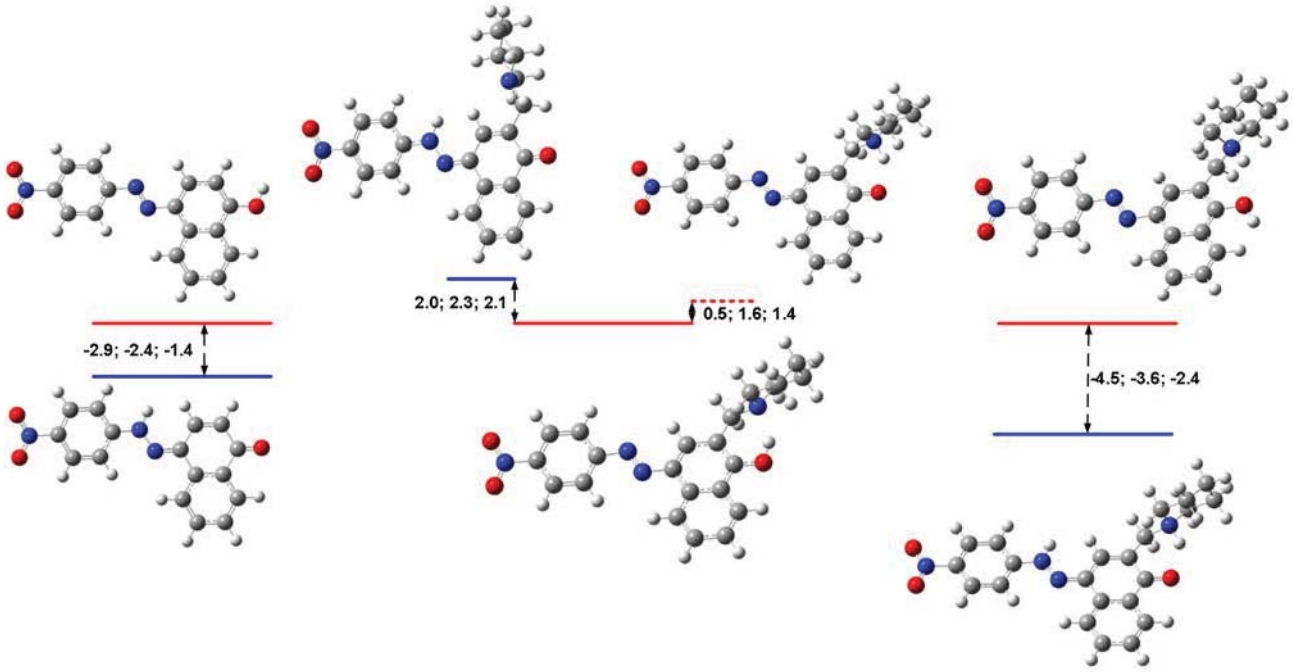

Figure S27: Change of the relative energy (M06-2X/def2-TZVP) of the tautomers in acetonitrile (PCM field) of the parent compound **8** (left), **4** (center) and **4H**$^+$ (right). The values of ΔE, ΔE+ZPE and ΔΔG are given in kcal/mol units.

Table S1: Most important crystal data and structure refinement parameters for **2**- **4**.

Compound reference	**2**	**3**	**4**
Chemical formula	$C_{23}H_{25}N_3O_2$	$C_{23}H_{22}N_4O$	$C_{22}H_{22}N_4O_3$
Formula Mass	375.46	370.45	390.44
Crystal system	Monoclinic	Triclinic	Triclinic
a/Å	34.716(8)	5.1014(8)	5.2175(7)
b/Å	5.994(4)	11.5731(17)	10.7215(16)
c/Å	20.442(6)	16.653(3)	17.295(3)
α/°	90	92.321(12)	82.197(12)
β/°	105.63(2)	93.662(13)	81.572(12)
γ/°	90	101.162(12)	89.056(12)
Unit cell volume/Å^3	4096(3)	961.2(3)	948.1(2)
Temperature/K	290(2)	200(2)	200(2)
Space group	*C*2/*c*	$P\bar{1}$	$P\bar{1}$
No. of formula units per unit cell, *Z*	8	2	2
Radiation type	MoKα	CuKα	MoKα
Absorption coefficient, μ/mm^{-1}	0.079	0.640	0.093
No. of reflections measured	7696	11643	12143
No. of independent reflections	4030	3169	3343
R_{int}	0.0833	0.0763	0.1473
Final R_1 values ($I > 2\sigma(I)$)	0.0564	0.0439	0.0605
Final $wR(F^2)$ values ($I > 2\sigma(I)$)	0.1167	0.1134	0.1530
Final R_1 values (all data)	0.181	0.0936	0.1476
Final $wR(F^2)$ values (all data)	0.1614	0.1360	0.1832
Goodness of fit on F^2	0.945	0.978	0.842

Table S2. Observed and calculated (PBE0/6-31G**) absorption maxima of compounds **1**-**8** in acetonitrile.

Structure	λ_{max} [nm]		
	observed	calculated	predicted*
1E	417	428	419
1K		452	
1EH$^+$		403	
1KH$^+$	495	475	477
1ZW		462	
5E	408	414	401
5K	468	450	446
2E	419	434	426
2K		484	
2EH$^+$		417	
2KH$^+$	517	516	528
2ZW		464	
6E	412	422	411
6K	495	484	488
3E	444	462	561
3K		449	
3EH$^+$		430	
3KH$^+$	472	472	473
3ZW	555	505	514
7E	429	446	441
7K	459	446	441
4E	466	496	503
4K		460	
4EH$^+$		450	
4KH$^+$	472	476	478
4ZW	593	561	584
8E	435	475	477
8K	468	456	453

* Predicted using the linear regression between observed and calculated values given in Figure S25.